

NOAA Technical Memorandum NMFS



JANUARY 2008

AN ASSESSMENT OF THE ACCURACY AND PRECISION OF LOCALIZATION OF A STATIONARY SOUND SOURCE USING A TWO-ELEMENT TOWED HYDROPHONE ARRAY

Shannon Rankin

Jay Barlow

Julie Oswald

NOAA-TM-NMFS-SWFSC-416

U.S. DEPARTMENT OF COMMERCE
National Oceanic and Atmospheric Administration
National Marine Fisheries Service
Southwest Fisheries Science Center

The National Oceanic and Atmospheric Administration (NOAA), organized in 1970, has evolved into an agency which establishes national policies and manages and conserves our oceanic, coastal, and atmospheric resources. An organizational element within NOAA, the Office of Fisheries is responsible for fisheries policy and the direction of the National Marine Fisheries Service (NMFS).

In addition to its formal publications, the NMFS uses the NOAA Technical Memorandum series to issue informal scientific and technical publications when complete formal review and editorial processing are not appropriate or feasible. Documents within this series, however, reflect sound professional work and may be referenced in the formal scientific and technical literature.



NOAA Technical Memorandum NMFS

This TM series is used for documentation and timely communication of preliminary results, interim reports, or special purpose information. The TMs have not received complete formal review, editorial control, or detailed editing.

JANUARY 2008

AN ASSESSMENT OF THE ACCURACY AND PRECISION OF LOCALIZATION OF A STATIONARY SOUND SOURCE USING A TWO-ELEMENT TOWED HYDROPHONE ARRAY

Shannon Rankin¹, Jay Barlow¹, and Julie Oswald²

¹NOAA, National Marine Fisheries Service
Southwest Fisheries Science Center
8604 La Jolla Shores Drive
La Jolla, California, USA 92037

²Scripps Institution of Oceanography
University of California, San Diego
La Jolla, California 92093

NOAA-TM-NMFS-SWFSC-416

U.S. DEPARTMENT OF COMMERCE

Carlos M. Gutierrez, Secretary

National Oceanic and Atmospheric Administration

VADM Conrad C. Lautenbacher, Jr., Undersecretary for Oceans and Atmosphere

National Marine Fisheries Service

James W. Balsiger, Acting Assistant Administrator for Fisheries

CONTENTS

List of Tables.....	3
List of Figures.....	3
Abstract.....	4
Introduction.....	5
Methods.....	5
Results.....	8
Discussion	9
Acknowledgments.....	12
Literature Cited.....	12

LIST OF TABLES

Table 1.	Signal source levels as a function of frequency.....	14
Table 2.	Results from the post-processing angle experiment.....	15
Table 3.	Results from the four-angle post-processing localization experiment.....	16
Table 4.	Results from the six-angle post-processing localization experiment.....	17
Table 5.	Results of the post-processing angle experiment.....	18
Table 6.	Results from the post-processing localization experiment...	19

LIST OF FIGURES

Figure 1.	Spectrograph of the three synthesized whistles.....	20
Figure 2.	Spectrograph of whistles with measurement parameters...	20
Figure 3.	Plot of real-time localization of sound using Whaltrak.....	21
Figure 4.	Changes in bearing angles from array to sound source.....	22
Figure 5.	Standard deviation of measurements for angle experiment..	23
Figure 6.	Localization experiment trials using 4 and 6 angles.....	24
Figure 7.	Whaltrak plot of angles during trial 2.....	25
Figure 8.	Whaltrak plot of angles during trial 19.....	26
Figure 9.	Whaltrak plot of angles during trial 29.....	27
Figure 10.	Whaltrak plot of angles from sperm whale detection.....	28
Figure 11.	Whaltrak plot of angles from dolphin school.....	29

ABSTRACT

An experiment to determine the accuracy of acoustic localization of a stationary sound source was performed during a recent Southwest Fisheries Science Center cetacean abundance survey. Synthesized whistles were transmitted via an underwater transducer deployed from a small boat. Signals were received using a 3-element hydrophone array towed 300 m behind a large research vessel. Bearings to the sound source were determined based on the time-delay of the signal arrival at two of the hydrophone elements. Localization was estimated by visually inspecting the convergence of bearing angles to the source. The accuracy of bearings and localizations improved as the ship approached the sound source. Bearing angles were imprecise when the bearings were less than 15 degrees from the ship's heading, and localizations were problematic when the sound source was less than 30 degrees from the ship's heading. When bearing angles were greater than 15 degrees, the standard deviation of repeated measures was typically less than one degree.

INTRODUCTION

Southwest Fisheries Science Center (SWFSC) has been conducting shipboard line-transect surveys of marine mammals since the 1970s (Kinzey et al. 2000), and incorporated the use of passive acoustic detection methods for cetacean in 2000 (Rankin and Barlow, manuscript). The purposes of the passive acoustics component were to determine whether the addition of acoustic detection can lead to more accurate cetacean population size estimates and to record sounds from cetaceans in order to study their vocal behavior. Passive acoustic detection of cetacean schools is not limited by light conditions and can potentially be used to survey when visual observations are limited by darkness or some weather conditions (Thomas et al. 1986). The location of vocalizing cetacean schools must be estimated to determine their position relative to the ship and to distinguish large, spread out schools from smaller consolidated schools when vocalizations are continuous. Likewise, in order to attribute vocalizations to a specific cetacean school, it is imperative we precisely determine its location.

We use a simple method for acoustic localization of cetacean vocalizations based on the convergence of successive bearing angles over time, where bearing angles are determined using the time delay of arrival of a signal detected by two closely-spaced hydrophone elements in a towed array. This method has been used by SWFSC for seven field seasons, and we have found a good agreement between the locations of cetacean sightings determined by both visual and acoustic methods. However, we have never empirically tested the accuracy or precision of this acoustic localization method on an object of known location. In this experiment, we use a stationary sound source with known location to quantify the variation of individual angles and estimated locations using this acoustic method.

METHODS

This experiment took place in an area of low marine mammal density during the 2006 *Stenella* Abundance Research (STAR) survey in the eastern tropical Pacific Ocean. A

small rigid hull inflatable boat (RHIB) was stationed 6 nmi ahead of the NOAA ship R/V *McArthur II*. The RHIB was allowed to drift, and its location was recorded every minute using a portable GPS. An underwater transducer was deployed from the RHIB for playback of synthesized whistles, which were localized by an acoustician using a towed hydrophone array on the *McArthur II*.

To avoid the inadvertent exposure of cetaceans to these test sounds during our experiment, we monitored for the presence of any cetaceans using visual and acoustic methods. Three experienced visual observers searched for marine mammals from the flying bridge of the *McArthur II* using two pairs of 25 X binoculars and naked eye. Two observers also maintained a 360° search for marine mammals from the RHIB. The towed hydrophone array was monitored for cetacean vocalizations during the experiment. To mitigate exposure to playback sounds, the experiment would have been postponed if any cetaceans had been detected within 5 nmi of the *McArthur II* by visual and/or acoustic methods. None were seen or heard during the experiment.

Synthesized whistles were transmitted using a spherical, omni-directional transducer (Innovative Transducer Corporation ITC-1001) deployed from the RHIB using 16 m of cable. A sea anchor was used to limit the RHIB's rate of wind drift; nonetheless drift caused a 45° cable angle, putting the hydrophone at an estimated depth of 11.3 m. Synthesized whistles were generated using a MatLab code and recorded to a CD. The whistles consisted of three different 1-s frequency sweeps (2-20 kHz, Fig. 1). Signals were recorded with constant amplitude for all frequencies and were played back continuously every 1-2 s using a CD player with the volume on the maximum setting. The signal from the CD player (73 mV-rms, -22.7 dB-V) was amplified with a 12-V Sony 1200-watt car stereo amplifier (flat frequency response to 32 kHz; fixed gain 47.1 dB). The output voltage from the amplifier (16.6 V-rms, 24.4 dB-V) was sent directly to the ITC-1001 transducer. The acoustic source level varied with frequency according to the transmit voltage response of this transducer from 147 dB re: 1 μ Pa at 4 kHz to 172 dB re: 1 μ Pa at 16 kHz (Table 1).

A three-element hydrophone array was towed 300 m behind the *McArthur II* at an average depth of 11 m while traveling at a speed of ~ 10 knots (18.5 km hr^{-1}). Only the first two hydrophones, separated by a distance of 3.9 m, were used for localization. The frequency sensitivity of these hydrophones was flat from 500 Hz to 40 kHz (± 3 dB at -165 dB re: $1 \mu\text{Pa}$). Signals from the hydrophones were equalized using a Mackie Mixer and recorded to a Tascam 8 channel Hi-8 digital recorder (sample rate of 48 kHz). Sounds were also digitized using a laptop computer and a National Instruments data acquisition card (NI-DAQ 6062-E) for real-time localization.

Received signals were processed and displayed in real-time digital using the program ISHMAEL (Mellinger 2001). An “array” file, indicating hydrophone spacing, and speed of sound (calculated from sea surface temperature and sea surface salinity provided by a flow-through system on the *McArthur II*) were provided to ISHMAEL to allow for accurate localizations. The “phone-pair” bearing estimation algorithm in ISHMAEL was used to determine bearing angles to the sound source. Bearing angles were plotted to Whaltrak, a mapping program that also logs time-stamped GPS locations. Successive bearing angles were plotted to Whaltrak as the ship progressed towards the sound source. Location of the sound source was visually estimated based on the convergence of these bearing angles (with left/right ambiguity). These methods were used to obtain estimated angles and locations of the sound source in real-time, and for two post-processing experiments which examined variation in estimated angles and locations.

An angle experiment was performed to examine variability in individual angles obtained using the phone-pair bearing algorithm in ISHMAEL. Once every minute, a series of four angle selections was obtained from each of the three synthesized whistles (Fig.2). The bearing angle for each of these angle selections was estimated in ISHMAEL and compared with the angles obtained in real-time and the true angles to the sound source at that time. An average of the four bearing angles was determined for each synthesized whistle for each minute; this average bearing angle was used in the localization experiment.

A localization experiment was performed to examine variation in the angle and distance to an estimated location of the sound source. In this experiment we used Whaltrak to plot the average of a series of 4 or 6 angles measured every two minutes. Each successive trial began one minute after the previous, for a total of 34 trials (using 4 angles) and 26 trials (using 6 angles). For example, the first trial used the average estimated bearing angle obtained at 10:02, 10:04, 10:06, and 10:08 (for 4 angles). The second trial used angle estimates obtained at 10:03, 10:05, 10:07, and 10:09. The location was estimated based on convergence of these angles on the Whaltrak plot, and the angle and distance from the ship to the estimated location were calculated in Whaltrak. These measurements were compared to the true location of the sound source at the time of the final angle plotted for that trial plus one minute (to account for approximate time required for estimating location in the field).

RESULTS

The RHIB was deployed in an area of low cetacean density at 2.757° N latitude and 109.687 ° W longitude, and was positioned at a point roughly 6 nmi ahead and 1 nmi off the trackline of the *McArthur II*. The sea anchor became entangled during deployment, allowing the RHIB to drift with the wind. The location of the RHIB was logged with a GPS every minute, and the drift rate was calculated at approximately 2 knots. The location of the *McArthur II* was logged by the GPS input in Whaltrak once every five minutes, with additional GPS updates logged for each comment and plotted bearing angle. The ships' heading was 296 ° (± 2 degrees) and the speed was 10 knots (± 0.2 knots) during the experiment.

The plot of the real-time acoustic localization of the sound source showed that it passed the beam of the ship at a distance of 1.2 nmi at 10:34 (Fig. 3). The visual observers independently confirmed that the RHIB passed the beam of the ship at 10:34 and estimated its distance as 1.1 nmi using binocular reticles. The true relative location of the RHIB at 10:34 was 92 degrees to port at a distance of 1.05 nmi (Table 5, 6).

The measurements for the post-processing angle experiment are shown in Table 2 and Figure 4. The difference between the measured angles (real-time and angle experiment) and the true angles decreased as the sound source passed alongside the *McArthur II* (Table 5, Fig. 4). The mean of the measured acoustic bearing angles from the angle experiment more closely matched the true angles than the bearing angles obtained in real-time (Table 5, Fig. 4). Initially, when the sound source was ahead of the ship (true bearing angle was less than 15 degrees), the standard deviation in measured angles was high (3.57 to 5.43 degrees, Fig. 5). However, the standard deviation decreased substantially (to less than 2.0 degrees) at 10:11, when the sound source was 15 degrees to port and 3.3 nmi from the *McArthur II* (Table 2, Fig. 5).

The data used for the post-processing localization experiment are shown in Table 3 (4 angles) and Table 4 (6 angles). The precision of localizations improved as the *McArthur II* approached the sound source (Table 6, Fig. 6). For localizations where all angles were less than 30 degrees (trials 1-13), a general lack of bearing angle convergence impedes a precise visual estimation of a location (Fig. 7A). This increased error in the estimated angle and distance to the sound source was found for trials using both 4 and 6 angles (Fig. 6). As angles increased to greater than 45 degrees, the ability to identify convergence using only four angles became possible (Fig. 8A). The increase in accuracy of the estimated angle and distance to the sound source at 10:23 (Table 6) coincides with a rapid increase in the change of bearing angles (Fig. 4). As the sound source passed the beam, the ability to estimate the point of convergence of the bearing angles increased even more (Fig. 9A). For each of these trials, a second Waltrak plot was created using the true bearing angles to the sound source (Fig. 7B, 8B, and 9B).

DISCUSSION

Due to its position behind the ship, a towed hydrophone array is at an inherent disadvantage for detecting sounds in front of the ship. Propeller cavitation leaves a trail of bubbles which masks sounds and may act as a physical barrier to sound sources directly ahead of the ship. Likewise, the ship hull may also act as a barrier to sounds

ahead of the ship, and engine noise masks lower frequency sounds. Acoustic localization depends not only on the initial detection of these sounds, but also on the accuracy of individual bearing angles, and on the precision of the convergence of these angles. Specifically, the errors inherent in these methods include the accuracy of the bearing angles, the ‘tightness’ of the convergence, and the movement of the sound source over time.

In an examination of a subset consisting of three years of acoustic monitoring, we have found that initial acoustic detections of delphinids are seldom made within 12° of the bow of the ship (Rankin and Barlow, manuscript). Although the synthesized whistles in this experiment could be easily detected when the signal was initiated at 11° and 4.23 nmi ahead of the ship, the accuracy of these initial acoustic bearing angles was low, and the variation in measured angles was high. Our results show that for our methods, precise estimates of angle (SD < 1.0 degree) are only possible at angles greater than 15 degrees (Fig. 5). In addition, bearing angles are accurate for a specific point, and any delay in plotting bearing angles naturally decreases the accuracy as the ship continually moves in relation to the sound source.

A ‘tight’ convergence of bearing angles is necessary for a precise estimation of the sound source location using these methods. Tight convergences occur with accurate bearings to a single animal and/or a group of closely associated animals (Fig. 10). Assuming sufficient plotting of accurate angles, a ‘loose’ convergence may indicate that the sound source itself is spread-out, or it is moving (Fig. 11). Inaccurate bearing angles will result in a poor or no convergence. Monitoring the range in the bearing angles obtained, and the change in these angles over time, will help identify if the vocalizing cetaceans are closely or loosely associated. In this study, the sound emanated from a single source, which would ideally allow for a tight convergence of bearing angles.

Unfortunately, our sound source, drifted at a speed of 2 knots, which likely contributed to at least some of the variation in the location estimation. This drift rate would result in a displacement of 0.26 nmi (493 m) during any given post-processing location experiment

trial using 4 angles, and a displacement of 0.33 nmi (617 m) during trials using 6 angles. For location estimation using 6 angles, all distance estimates using angles between 42 and 118 degrees fell within this error range (Table 6).

In the post-processing localization experiment, an attempt was made to estimate the location of the sound source using a total of only four or six bearing angles separated by a maximum time period of 10 minutes. For angles ahead of the ship (less than 30 degrees), the small number of angles used in this experiment may not be sufficient to allow for convergence (Fig. 7). As the angles increase, the convergence becomes more definitive, and errors in individual angles have less of an impact on the estimated location (Fig. 9). As sound source passes the beam of the ship, the convergence becomes more evident, making the estimation of the location more accurate. Therefore, a greater number of angles are needed when the sound source is ahead of the ship and fewer are needed as the sound source approach the beam of the ship.

We would expect estimated angles to be symmetrically distributed about the true; however, this was not the case. The estimated angles obtained in real-time and during the post-process angle experiment were consistently greater than the true angles between 10:11 (15°) and 10:28 (52°, Table 5). The cause of this bias in the measured angles (real-time and angle experiment) are unknown, and should be examined in the future. It should be noted that a bias of this type in the *estimated angle to the location* of the sound source could be explained by an inaccurate measurement of the distance between the ship and the first hydrophone in the array. This would not, however, explain the differences seen in the *measured angles*.

This study confirms the accuracy of acoustic methods of localization for sound sources that are detected in close proximity to the ship, assuming that bearing angles greater than 30 degrees are obtained. Location estimation may be negatively affected by a sound source that is spread-out or moving, or for which consistent bearing angles past 30 degrees cannot be obtained. Determination of a location for any sound source is best obtained as it passes the beam of the ship.

Future research should examine the possible impact the ship has on detection of sound sources ahead of the ship, and use alternate synthetic signals to examine the affect of the frequency, frequency shift (slope), and the signal intensity on bearing angle calculation using time-delay (phone-pair bearing). This experiment should be repeated using a truly stationary sound source to increase our ability to test the accuracy of this methodology. Additional trials at varying distances would allow an independent examination of the localization accuracy based on the angle of the sound source as well as the distance of the sound source.

ACKNOWLEDGMENTS

This experiment could not have been performed without the help of the officers and crew of the NOAA ship R/V *McArthur II*. Special thanks to the scientists and the principal investigator for the STAR 2006 survey, Lisa Ballance, for their cooperation. Liz Zele provided valuable acoustics assistance during this experiment and the whole of the STAR 2006 survey. This manuscript was improved by helpful reviews by Tom Norris and Sue Moore. Funding was provided by the U. S Navy.

LITERATURE CITED

- Kinzey, D., P. Olson, and T. Gerrodette. 2000. Marine mammal data collection procedures on research line-transect surveys by the Southwest Fisheries Science Center. NOAA Administrative Report LJ-00-07C, available from SWFSC, 8604 La Jolla Shores Dr, La Jolla, CA 92037.
- Mellinger, D. K. 2001. ISHMAEL 1.0 User's Guide. NOAA Technical Memorandum OAR PMEL-120, available from NOAA/PMEL, 7600 Sand Point Way NE, Seattle, WA 98115-6349.

Rankin, S. and J. Barlow. 2006. Acoustic Studies of Marine Mammals During Shipboard Population Surveys in the Eastern Tropical Pacific, Around Hawai'i, and Off the West Coast of the United States. Manuscript, 64p.

Thomas, J. A., F. A. Awbrey, and S. R. Fisher. 1986. Use of acoustic techniques in studying whale behaviors. *In: Behavior of Whales in Relation to Management*, G. P. Donovan, ed. Report to the Int. Whal. Comm., Special Issue 8 (pp. 121-138).

Table 1. Signal source levels as a function of frequency as calculated from the factory calibration sensitivity (transmit voltage response) of the ITC-1001 transducer and the 16.6 V-rms amplifier output. The transducer was not calibrated below 4 kHz, but source levels would be relatively small.

Frequency (kHz)	Transmit Voltage Response	Source Level (dB re 1 μ Pa)
4	122.3	146.7
5	125.5	149.9
6	127.9	152.3
7	130.3	154.7
8	132.2	156.6
9	134.5	158.9
10	136.4	160.8
11	141.6	166.0
12	144.3	168.7
13	145.8	170.2
14	146.8	171.2
15	147.2	171.6
16	147.6	172.0
17	147.5	171.9
18	147.2	171.6
19	147.1	171.5
20	147.0	171.4

Table 2. Results from post-processing angle experiment. Four angle measurements (A, B, C, D from Fig. 2) were taken from three different synthesized whistles (1, 2, 3 from Fig.1) for each minute of the experiment. All angle values are in degrees. The range, mean, and standard deviation are calculated from all measured whistles.

Time	Acoustic Bearing Angle												Range	Mean
	1A	1B	1C	1D	2A	2B	2C	2D	3A	3B	3C	3D		
10:02	4	15	18	21	8	15	8	15	8	17	13	18	4-21	13.3
10:03	4	15	18	17	4	15	15	18	18	11	13	15	4-18	13.6
10:04	8	8	11	11	8	17	15	17	8	15	13	15	8-17	12.2
10:05	15	15	18	17	17	15	13	18	8	17	17	11	8-18	15.1
10:06	8	20	13	4	8	17	11	4	11	18	13	18	4-20	12.1
10:07	8	20	11	4	11	17	17	8	4	17	11	11	4-20	11.6
10:08	18	18	25	18	18	18	18	17	17	18	18	13	13-25	18.0
10:09	15	18	15	13	13	18	18	13	4	17	8	13	4-18	13.8
10:10	18	20	18	18	20	20	20	18	8	22	21	20	8-22	18.6
10:11	18	20	20	18	18	18	21	18	18	18	21	18	18-21	18.8
10:12	21	22	21	21	22	22	20	22	22	22	21	22	20-22	21.5
10:13	21	21	21	22	21	21	17	21	21	21	18	21	17-21	20.5
10:14	21	21	21	21	21	21	22	21	22	21	22	22	21-22	21.3
10:15	22	22	26	22	21	21	20	21	21	21	22	21	20-26	21.7
10:16	22	22	25	23	22	23	23	21	23	23	22	23	21-25	22.7
10:17	23	22	27	23	22	23	25	22	23	23	18	23	18-27	22.8
10:18	27	27	23	26	26	26	23	23	26	26	25	25	23-27	25.3
10:19	27	27	26	26	26	26	25	26	26	26	26	26	25-27	26.1
10:20	28	28	26	28	28	28	26	29	28	28	28	28	26-28	27.8
10:21	31	32	30	31	31	31	33	31	31	31	32	31	30-33	31.3
10:22	31	31	32	31	31	31	31	31	32	32	33	31	31-33	31.4
10:23	35	35	34	35	35	35	35	35	35	35	35	35	34-35	34.9
10:24	37	37	37	37	38	38	36	38	38	38	37	39	36-39	37.5
10:25	40	40	40	40	40	41	41	40	40	40	42	41	40-42	40.4
10:26	44	44	43	44	44	44	46	44	44	44	42	44	42-44	43.9
10:27	47	47	49	47	48	48	49	47	48	48	47	48	47-49	47.8
10:28	52	52	53	52	52	52	51	52	52	52	51	52	51-53	51.9
10:29	57	57	56	57	57	57	56	57	56	56	56	57	56-57	56.6
10:30	63	63	63	62	63	63	65	63	63	63	64	63	62-65	63.2
10:31	69	69	70	69	70	70	70	70	70	70	70	69	69-70	69.7
10:32	77	77	79	77	77	77	79	77	77	77	77	77	77-79	77.3
10:33	83	83	84	82	83	83	84	83	83	83	84	83	82-84	83.2
10:34	90	91	92	90	90	90	90	90	91	91	91	91	90-92	90.6
10:35	98	98	97	97	98	97	96	98	98	98	100	98	96-100	97.8
10:36	106	106	108	106	105	105	105	105	105	105	104	105	104-106	105.4
10:37	113	113	108	113	113	113	111	113	113	113	113	113	108-113	112.4
10:38	119	119	120	119	120	120	120	120	120	120	121	120	119-121	119.8
10:39	124	124	125	124	124	124	124	124	124	124	125	124	124-125	124.2
10:40	129	129	128	129	129	129	130	129	129	129	129	129	128-130	129.0
10:41	133	133	131	133	133	133	133	132	132	132	135	133	132-135	132.8

Table 3. Results from the four-angle post-processing localization experiment. Four angles separated by two minutes were obtained from the average of the post-processing angle experiment and were plotted in Whaltrak to determine an estimated location for the sound source. The angle and distance to this position were estimated using Whaltrak. All angles are in degrees and distances are in nautical miles.

Trial	Angle 1		Angle 2		Angle 3		Angle 4		Estimated	
	Time	Angle	Time	Angle	Time	Angle	Time	Angle	Angle	Distance
1	10:02	347	10:04	348	10:06	348	10:08	342	21	1.17
2	10:03	346	10:05	345	10:07	348	10:09	346	13	3.64
3	10:04	348	10:06	348	10:08	342	10:10	341	13	2.44
4	10:05	345	10:07	348	10:09	346	10:11	341	18	1.77
5	10:06	348	10:08	342	10:10	341	10:12	338	19	2.06
6	10:07	348	10:09	346	10:11	341	10:13	339	28	1.00
7	10:08	342	10:10	341	10:12	338	10:14	339	23	2.86
8	10:09	346	10:11	341	10:13	339	10:15	338	26	2.03
9	10:10	341	10:12	338	10:14	339	10:16	337	28	1.91
10	10:11	341	10:13	339	10:15	338	10:17	337	25	4.27
11	10:12	338	10:14	339	10:16	337	10:18	335	33	1.07
12	10:13	339	10:15	338	10:17	337	10:19	334	27	2.49
13	10:14	339	10:16	337	10:18	335	10:20	332	47	0.57
14	10:15	338	10:17	337	10:19	334	10:21	329	37	1.24
15	10:16	337	10:18	335	10:20	332	10:22	329	34	2.00
16	10:17	337	10:19	334	10:21	329	10:23	325	39	1.49
17	10:18	335	10:20	332	10:22	329	10:24	322	45	1.21
18	10:19	334	10:21	329	10:23	325	10:25	320	45	0.98
19	10:20	332	10:22	329	10:24	322	10:26	316	53	1.27
20	10:21	329	10:23	325	10:25	320	10:27	312	58	1.02
21	10:22	329	10:24	322	10:26	316	10:28	308	61	1.15
22	10:23	325	10:25	320	10:27	312	10:29	303	66	1.21
23	10:24	322	10:26	316	10:28	308	10:30	297	68	1.09
24	10:25	320	10:27	312	10:29	303	10:31	290	80	1.04
25	10:26	316	10:28	308	10:30	297	10:32	283	92	1.14
26	10:27	312	10:29	303	10:31	290	10:33	277	87	1.18
27	10:28	308	10:30	297	10:32	283	10:34	269	101	1.40
28	10:29	303	10:31	290	10:33	277	10:35	262	111	1.38
29	10:30	297	10:32	283	10:34	269	10:36	255	113	1.38
30	10:31	290	10:33	277	10:35	262	10:37	248	112	1.49
31	10:32	283	10:34	269	10:36	255	10:38	240	127	1.47
32	10:33	277	10:35	262	10:37	248	10:39	236	124	1.77
33	10:34	269	10:36	255	10:38	240	10:40	231	145	1.97
34	10:35	262	10:37	248	10:39	236	10:41	227	138	1.98

Table 4. Results from the six-angle post-processing localization experiment. Six angles separated by two minutes were obtained from the average of the post-processing angle experiment and were plotted in Whaltrak to determine an estimated location for the sound source. The angle and distance to this position were estimated using Whaltrak. All angles are in degrees and distances are in nautical miles.

Trial	Angle 1		Angle 2		Angle 3		Angle 4		Angle 5		Angle 6		Estimated	
	Time	Angle	Time	Angle	Time	Angle	Time	Angle	Time	Angle	Time	Angle	Angle	Distance
1	10:02	347	10:04	348	10:06	348	10:08	342	10:10	341	10:12	338	23	2.4
2	10:03	346	10:05	345	10:07	348	10:09	346	10:11	341	10:13	339	28	1.6
3	10:04	348	10:06	348	10:08	342	10:10	341	10:12	338	10:14	339	30	1.4
4	10:05	345	10:07	348	10:09	346	10:11	341	10:13	339	10:15	338	23	1.6
5	10:06	348	10:08	342	10:10	341	10:12	338	10:14	339	10:16	337	14	1.6
6	10:07	348	10:09	346	10:11	341	10:13	339	10:15	338	10:17	337	26	2.1
7	10:08	342	10:10	341	10:12	338	10:14	339	10:16	337	10:18	335	29	1.4
8	10:09	346	10:11	341	10:13	339	10:15	338	10:17	337	10:19	334	33	1.9
9	10:10	341	10:12	338	10:14	339	10:16	337	10:18	335	10:20	332	33	1.4
10	10:11	341	10:13	339	10:15	338	10:17	337	10:19	334	10:21	329	35	1.9
11	10:12	338	10:14	339	10:16	337	10:18	335	10:20	332	10:22	329	31	2.5
12	10:13	339	10:15	338	10:17	337	10:19	334	10:21	329	10:23	325	37	2.3
13	10:14	339	10:16	337	10:18	335	10:20	332	10:22	329	10:24	322	34	2.8
14	10:15	338	10:17	337	10:19	334	10:21	329	10:23	325	10:25	320	42	2.0
15	10:16	337	10:18	335	10:20	332	10:22	329	10:24	322	10:26	316	44	1.6
16	10:17	337	10:19	334	10:21	329	10:23	325	10:25	320	10:27	312	55	1.3
17	10:18	335	10:20	332	10:22	329	10:24	322	10:26	316	10:28	308	54	1.3
18	10:19	334	10:21	329	10:23	325	10:25	320	10:27	312	10:29	303	60	1.3
19	10:20	332	10:22	329	10:24	322	10:26	316	10:28	308	10:30	297	68	1.3
20	10:21	329	10:23	325	10:25	320	10:27	312	10:29	303	10:31	290	70	1.2
21	10:22	329	10:24	322	10:26	316	10:28	308	10:30	297	10:32	283	81	1.2
22	10:23	325	10:25	320	10:27	312	10:29	303	10:31	290	10:33	277	91	1.2
23	10:24	322	10:26	316	10:28	308	10:30	297	10:32	283	10:34	269	90	1.2
24	10:25	320	10:27	312	10:29	303	10:31	290	10:33	277	10:35	262	104	1.2
25	10:26	316	10:28	308	10:30	297	10:32	283	10:34	269	10:36	255	112	1.4
26	10:27	312	10:29	303	10:31	290	10:33	277	10:35	262	10:37	248	114	1.4

Table 5. Results of post-processing angle experiment. The average of the angles obtained in real-time and by post-processing was compared with the true angle to the sound source. The offset is the difference between estimated angle (real-time or post-processing mean) and the true angle. All angles are in degrees.

Time	<i>Real-Time</i>	<i>Angle Experiment</i>		<i>True</i>	Offset Post-Processing	
	Angle	Range	Mean	Angle	Real-time	Mean
10:04	14	8-17	12.2	11	3.0	1.2
10:05	17	8-18	15.1	11	6.0	4.1
10:06	-	4-20	12.1	12	-	0.1
10:07	14	4-20	11.6	12	2.0	-0.4
10:08	19	13-25	18.0	13	6.0	5.0
10:09	15	4-18	13.8	14	1.0	-0.3
10:10	20	8-22	18.6	14	6.0	4.6
10:11	23	18-21	18.8	15	8.0	3.8
10:12	23	20-22	21.5	16	7.0	5.5
10:13	22	17-21	20.5	17	5.0	3.5
10:14	21	21-22	21.3	18	3.0	3.3
10:15	-	20-26	21.7	19	-	2.7
10:16	25	21-25	22.7	20	5.0	2.7
10:17	-	18-27	22.8	21	-	1.8
10:18	28	23-27	25.3	22	6.0	3.3
10:19	-	25-27	26.1	24	-	2.1
10:20	32	26-28	27.8	25	7.0	2.8
10:21	28	30-33	31.3	27	1.0	4.3
10:22	-	31-33	31.4	30	-	1.4
10:23	35	34-35	34.9	32	3.0	2.9
10:24	38	36-39	37.5	34	4.0	3.5
10:25	-	40-42	40.4	38	-	2.4
10:26	43	42-44	43.9	42	1.0	1.9
10:27	-	47-49	47.8	47	-	0.8
10:28	50	51-53	51.9	52	-2.0	-0.1
10:29	57	56-57	56.6	58	-1.0	-1.4
10:30	65	62-65	63.2	64	1.0	-0.8
10:31	70	69-70	69.7	69	1.0	0.7
10:32	77	77-79	77.3	76	1.0	1.3
10:33	82	82-84	83.2	84	-2.0	-0.8
10:34	92	90-92	90.6	92	0.0	-1.4
10:35	100	96-100	97.8	100	0.0	-2.3
10:36	105	104-106	105.4	108	-3.0	-2.6
10:37	113	108-113	112.4	115	-2.0	-2.6
10:38	121	119-121	119.8	118	3.0	1.8
10:39	125	124-125	124.2	123	2.0	1.2
10:40	130	128-130	129.0	128	2.0	1.0

Table 6. Results from the post-processing localization experiment. The estimated angle and distance to the sound source using 4 and 6 angles were compared with the true angle and distance to the sound source. The location time was one minute past the final angle time used in the localization experiment. The offset was the estimated angle/distance subtracted from the true angle/distance, respectively. Angles are in degrees, and distances are in nautical miles.

Trial	Location Time	TRUE		4 Angle Estimate		6 Angle Estimate		4 Angle Offset		6 Angle Offset	
		Angle	Distance	Angle	Distance	Angle	Distance	Angle	Distance	Angle	Distance
1	10:09	14	3.6	21	1.2	-	-	7	-2.4	-	-
2	10:10	14	3.5	13	3.6	-	-	-1	0.2	-	-
3	10:11	15	3.3	13	2.4	-	-	-2	-0.9	-	-
4	10:12	16	3.2	18	1.8	-	-	2	-1.4	-	-
5	10:13	17	3.1	19	2.1	23	2.4	2	-1.0	6	-0.7
6	10:14	18	2.9	28	1.0	28	1.6	10	-1.9	10	-1.3
7	10:15	19	2.8	23	2.9	30	1.4	4	0.1	11	-1.4
8	10:16	20	2.7	26	2.0	23	1.6	6	-0.6	3	-1.1
9	10:17	21	2.5	28	1.9	14	1.6	7	-0.6	-7	-0.9
10	10:18	22	2.4	25	4.3	26	2.1	3	1.9	4	-0.3
11	10:19	24	2.3	33	1.1	29	1.4	9	-1.2	5	-0.9
12	10:20	25	2.1	27	2.5	33	1.9	2	0.4	8	-0.3
13	10:21	27	2.0	47	0.6	33	1.4	20	-1.4	6	-0.7
14	10:22	30	1.9	37	1.2	35	1.9	7	-0.6	5	0.0
15	10:23	32	1.8	34	2.0	31	2.5	2	0.2	-1	0.7
16	10:24	34	1.7	39	1.5	37	2.3	5	-0.2	3	0.6
17	10:25	38	1.5	45	1.2	34	2.8	7	-0.3	-5	1.3
18	10:26	42	1.4	45	1.0	42	2.0	3	-0.5	0	0.6
19	10:27	47	1.3	53	1.3	44	1.6	6	-0.1	-4	0.2
20	10:28	52	1.3	58	1.0	55	1.3	6	-0.2	3	0.0
21	10:29	58	1.2	61	1.2	54	1.3	3	0.0	-5	0.1
22	10:30	64	1.1	66	1.2	60	1.3	2	0.1	-4	0.1
23	10:31	69	1.1	68	1.1	68	1.3	-1	0.0	-1	0.2
24	10:32	76	1.1	80	1.0	70	1.2	4	0.0	-7	0.1
25	10:33	84	1.0	92	1.1	81	1.2	8	0.1	-4	0.1
26	10:34	92	1.1	87	1.2	91	1.2	-5	0.1	-2	0.1
27	10:35	100	1.1	101	1.4	90	1.2	1	0.3	-10	0.1
28	10:36	108	1.1	111	1.4	104	1.2	3	0.3	-4	0.1
29	10:37	115	1.2	113	1.4	112	1.4	-2	0.2	-3	0.2
30	10:38	118	1.2	112	1.5	114	1.4	-6	0.3	-4	0.1
31	10:39	123	1.3	127	1.5	-	-	4	0.1	-	-
32	10:40	128	1.4	124	1.8	-	-	-4	0.4	-	-

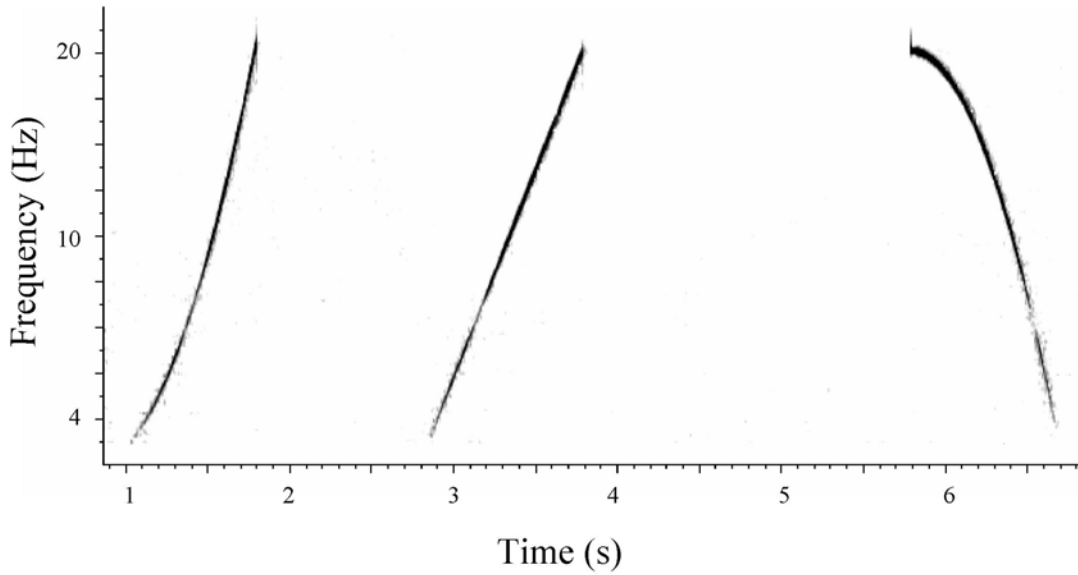


Figure 1. Spectrograph of the three synthesized whistles used in localization experiment.

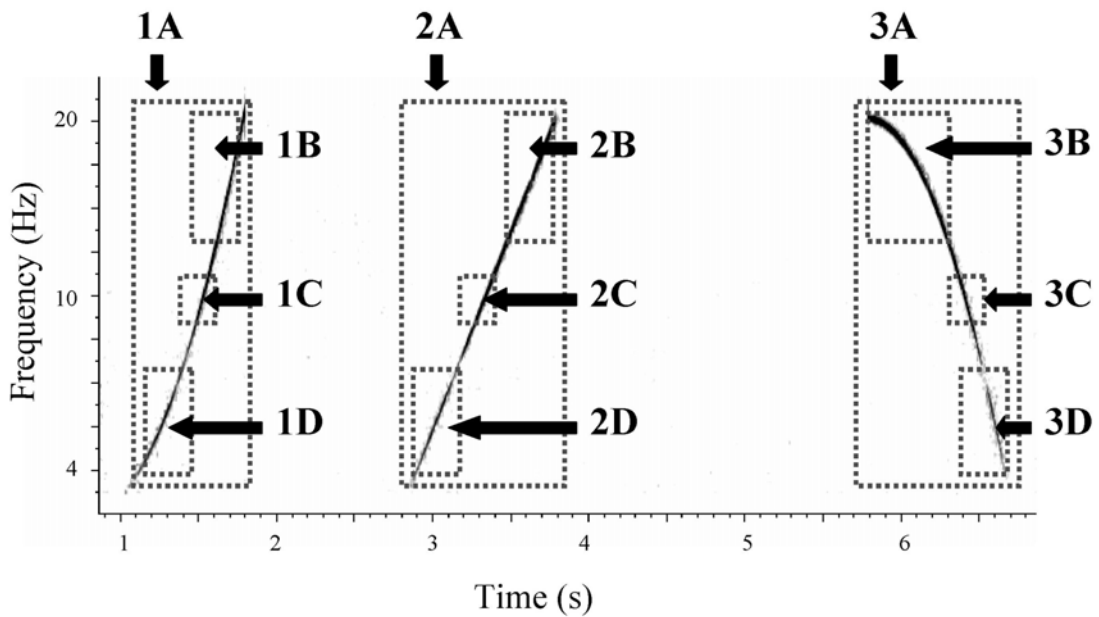


Figure 2. Spectrograph of three synthesized whistles used in localization experiment, with measurement parameters. For each whistle, four different selections were made for the phone-pair algorithm in ISHMAEL. Selection A (for each whistle 1-3) selected the entire whistle; selections B-D used smaller selections of the whistle.

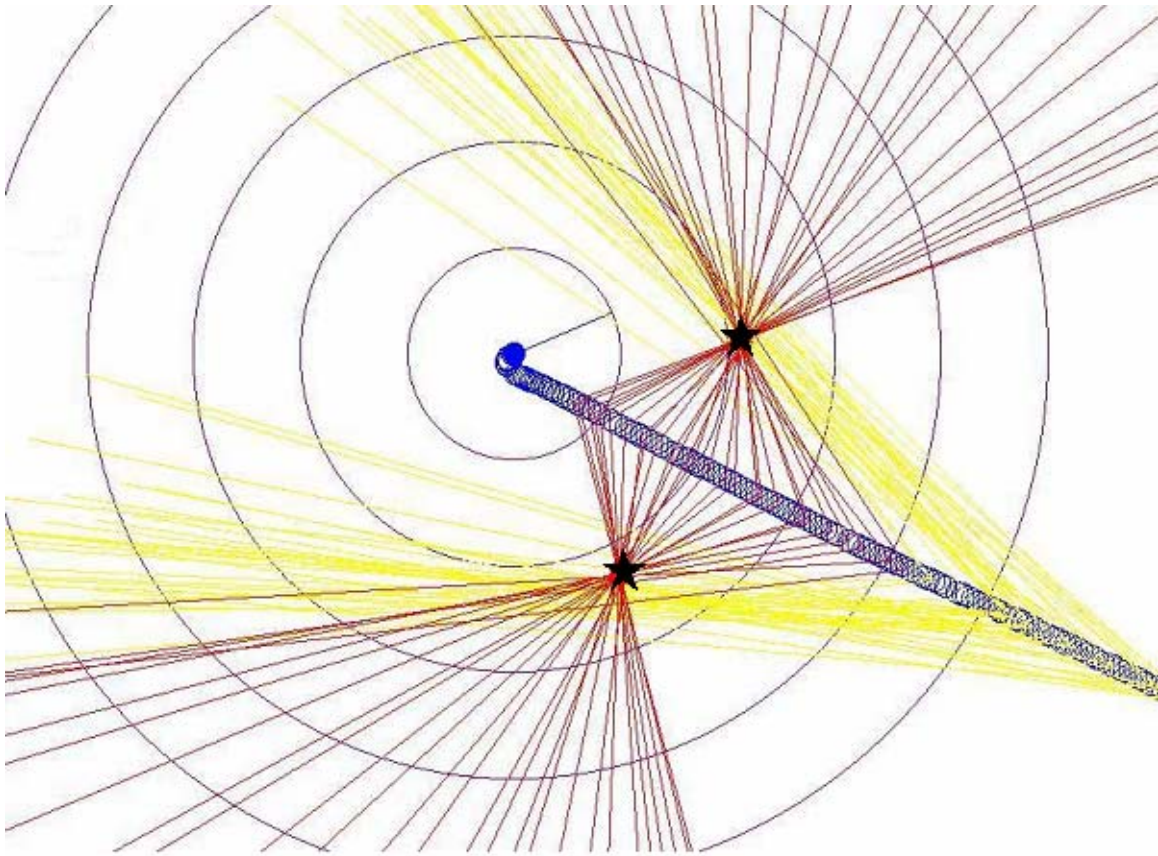


Figure 3. Plot of real-time localization of the sound source using the Whaltrak mapping software program. The ship's trackline is shown as overlapping open circles; current ship location is shown as closed blue circle. For reference, one nautical mile concentric rings surround the current location of the ship. Bearing angles provided by ISHMAEL are plotted in real-time (yellow = lines older than 20 minutes, red = lines plotted within 20 minutes). Black stars indicate the locations of the sound source as determined by the convergence of bearing angles plotted in real-time (with a left/right ambiguity).

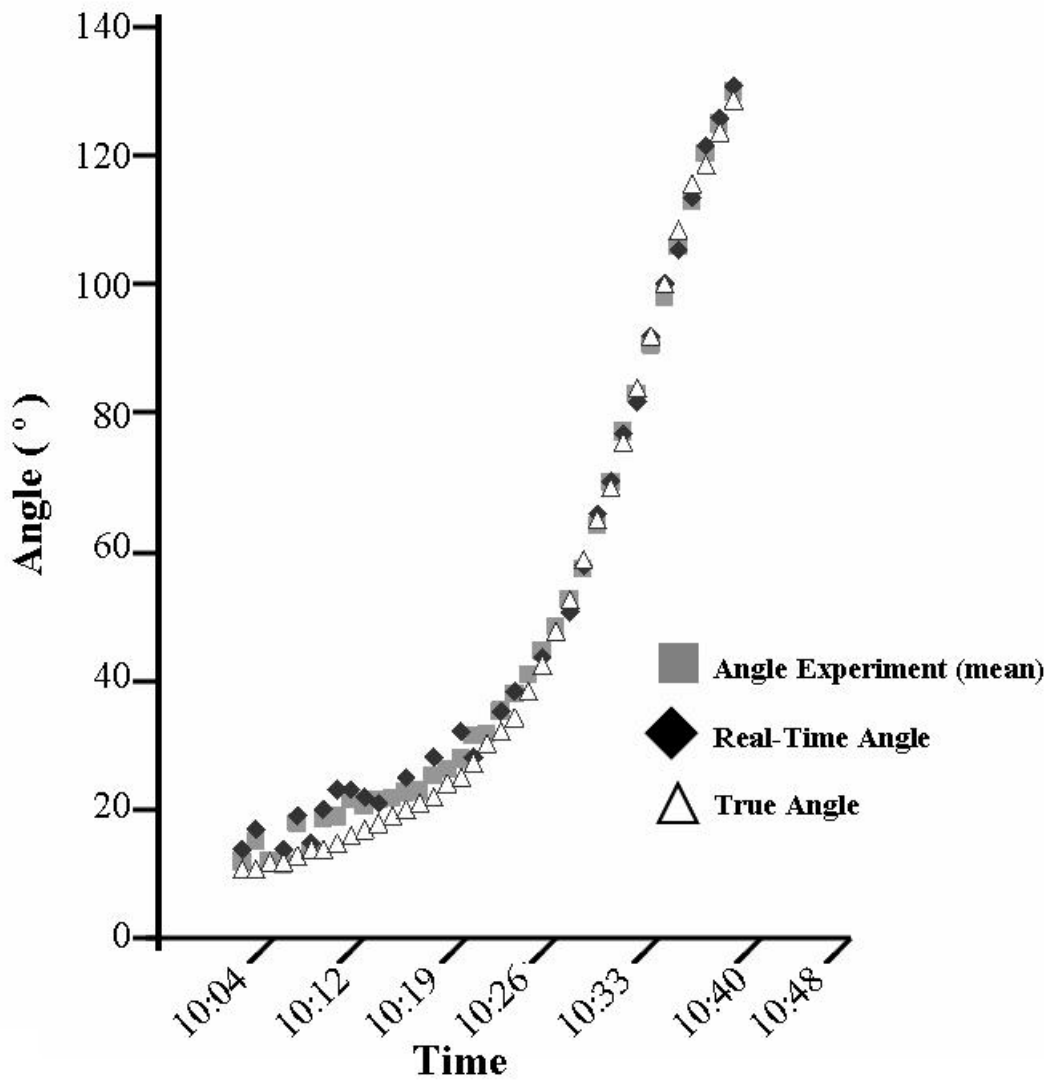


Figure 4. Changes in bearing angles from hydrophone array to sound source over time. True angles are shown as white triangles, angles obtained in real-time using the hydrophone array are shown as black diamonds, and the mean angles obtained from the angle experiment are shown as gray squares.

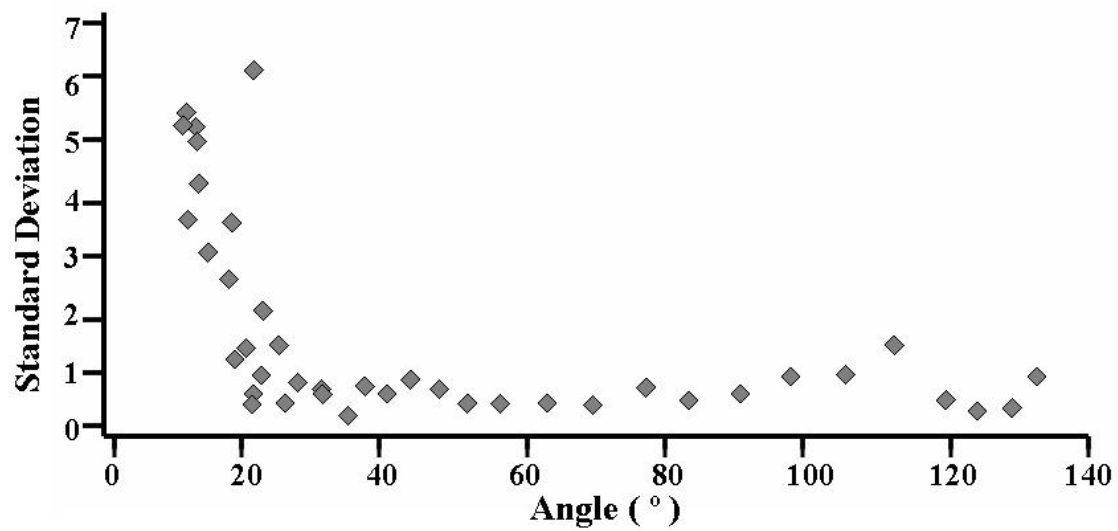


Figure 5. Standard deviation of measurements for angles measured in the angle experiment.

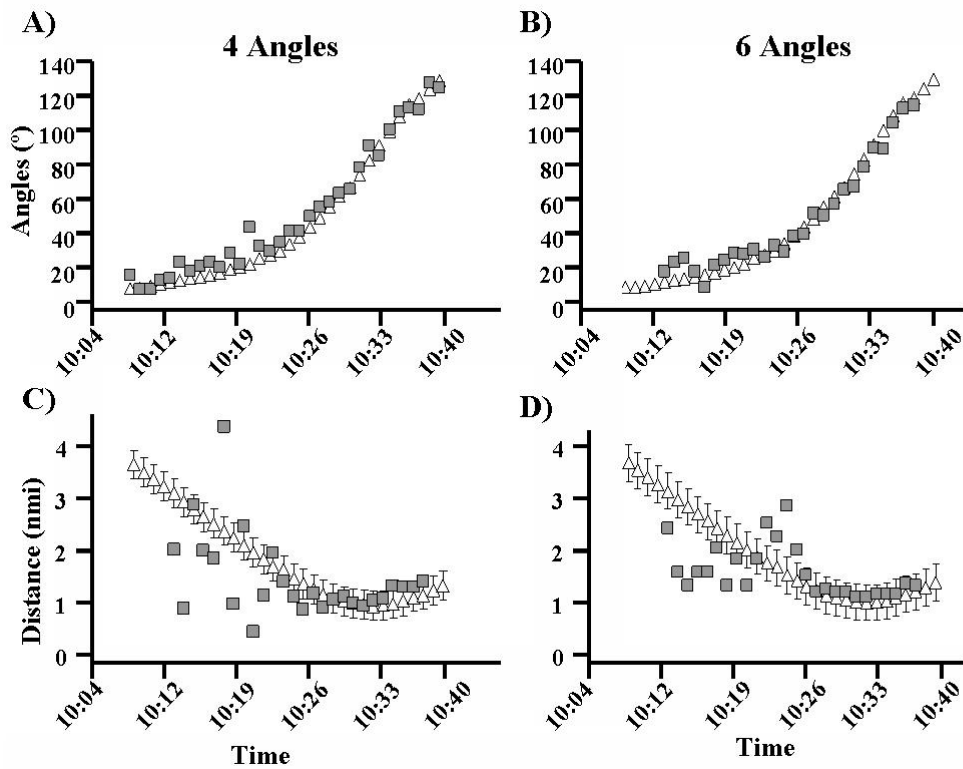
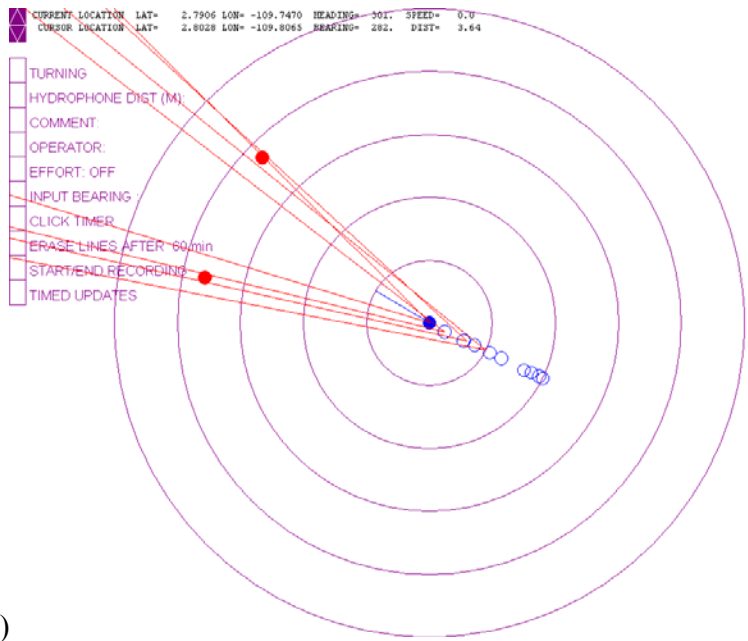
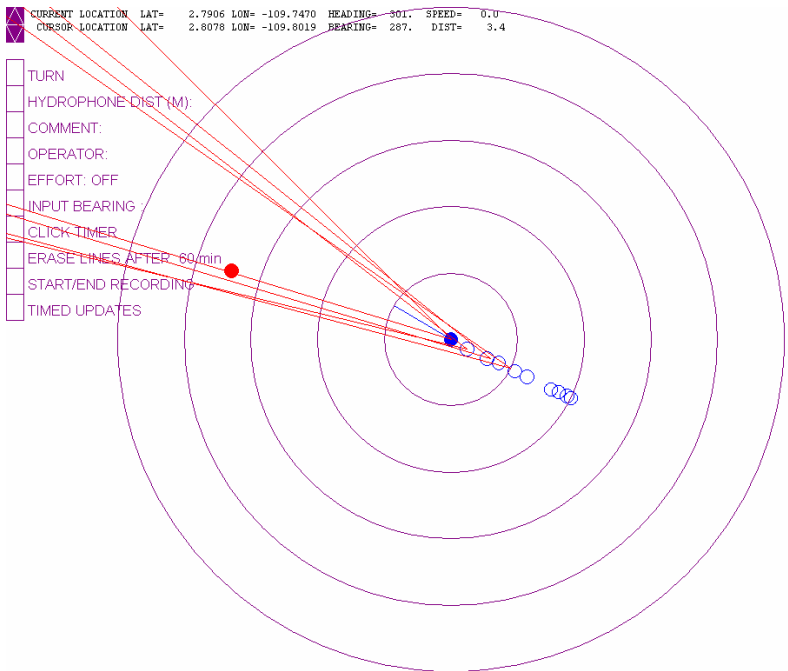


Figure 6. Localization experiment results for trials using 4 angles and 6 angles. Estimated angles over time for the 4-angle trials (A) and 6-angle trials (B) are shown as gray squares. True angles over time are shown as white triangles (A, B). Estimated distances to the sound source over time for the 4-angle trials (C) and 6-angle trials (D) are shown as gray squares. True distances to the sound source over time are shown as white triangles (C, D), with error bars showing range of drift of sound source during a given trial.

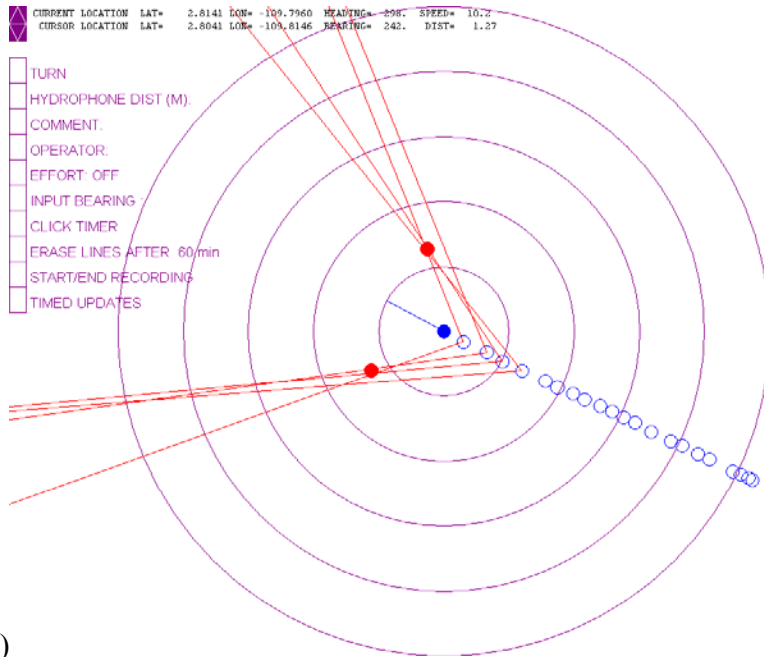


(A)

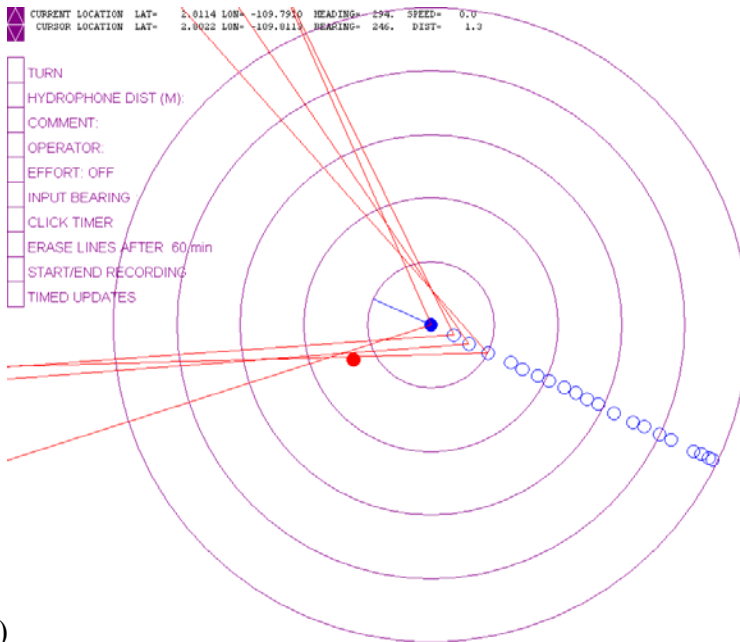


(B)

Figure 7. Whaltrak plot of angles during trial 2 from (A) post-processing localization experiment and (B) true angles. Red dots indicate estimated location of sound source using convergence of beamform angles (A) and true location of sound source (B). Minimal change in forward angles prevents the convergence of angles necessary for estimating a location to the sound source using these techniques.



(A)



(B)

Figure 8. Whaltrak plot of angles during trial 19 from (A) post-processing localization experiment and (B) true angles. Red dots indicate estimated location of sound source using convergence of beamform angles (A) and true location of sound source (B). Angle to sound source is greater and distance to sound source is decreased compared to earlier plots, resulting in an increase in accuracy of the acoustic estimation of the sound source. At 10:32, the sound source was estimated to be 53 degrees and 1.27 nmi from the ship. The true location of the sound source at this time was 47 degrees to the left of the ship and 1.34 nmi.

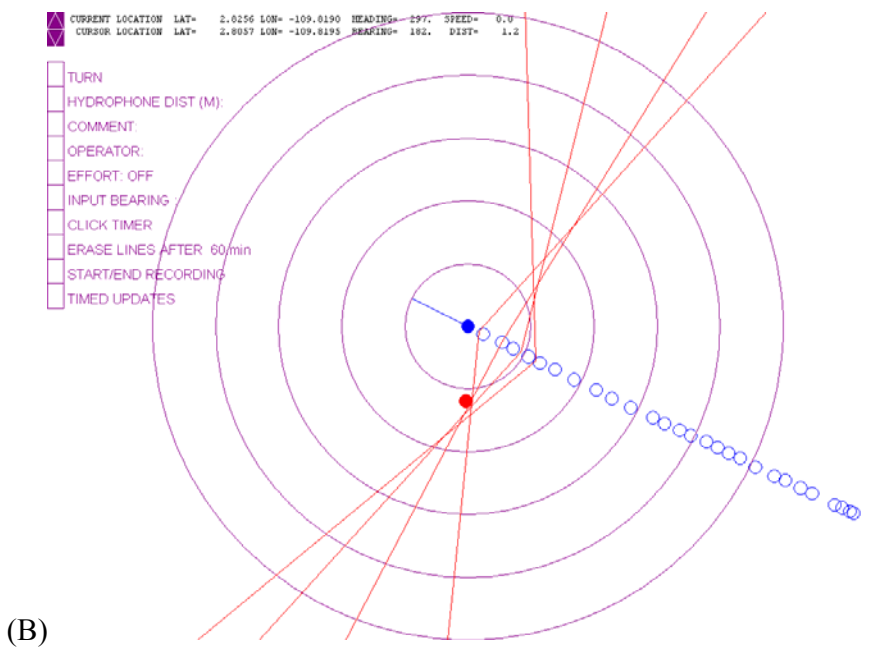
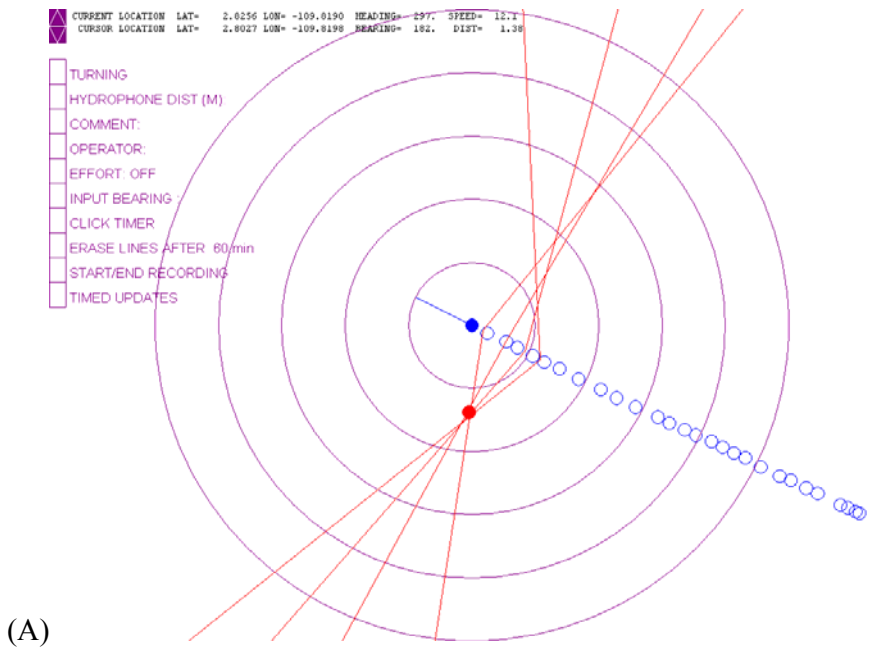


Figure 9. Whaltrak plot of angles during trial 29 from (A) post-processing localization experiment and (B) true angles. Red dots indicate estimated location of sound source using convergence of beamform angles (A) and true location of sound source (B). After the sound source passes the beam of the ship, it is easier for the acoustician to estimate the location to the sound source with high accuracy. At 10:37, the sound source was estimated to be at 113 degrees and 1.38 nmi from the ship. The true location of the sound source at this time was 115 degrees at 1.2 nmi.

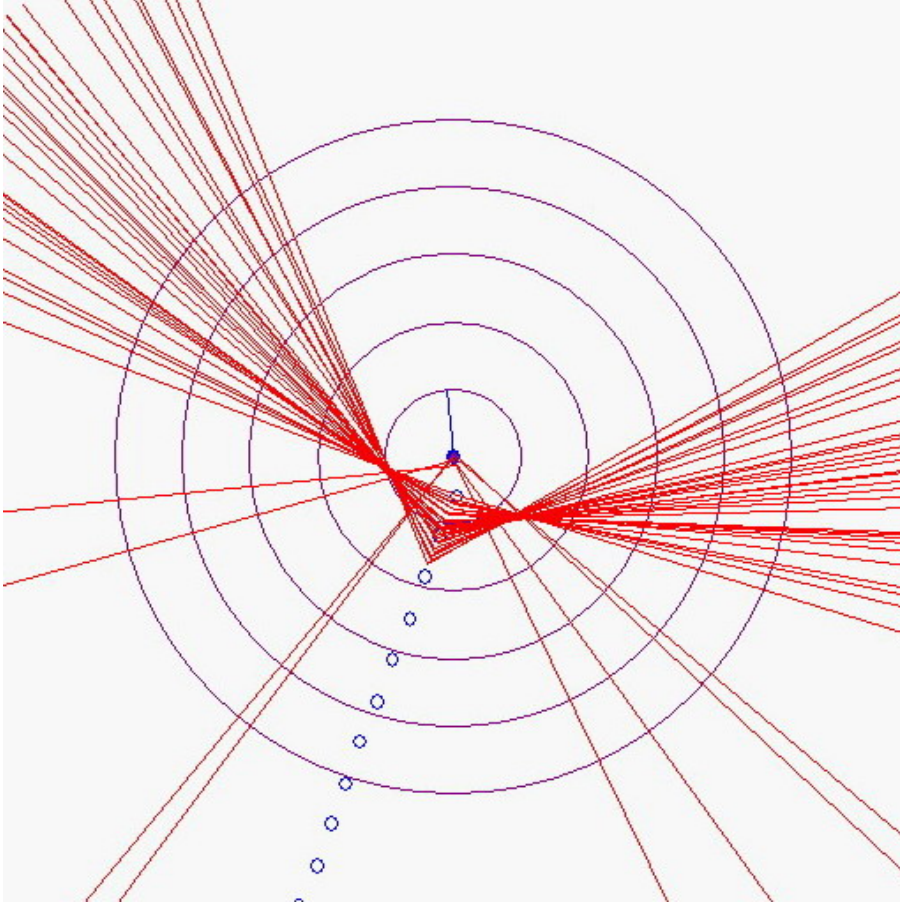


Figure 10. Whaltrak plot of angles obtained on a sperm whale detection, with a 'tight' convergence suggesting a location of a single vocalizing animal or a tight group of vocalizing animals.

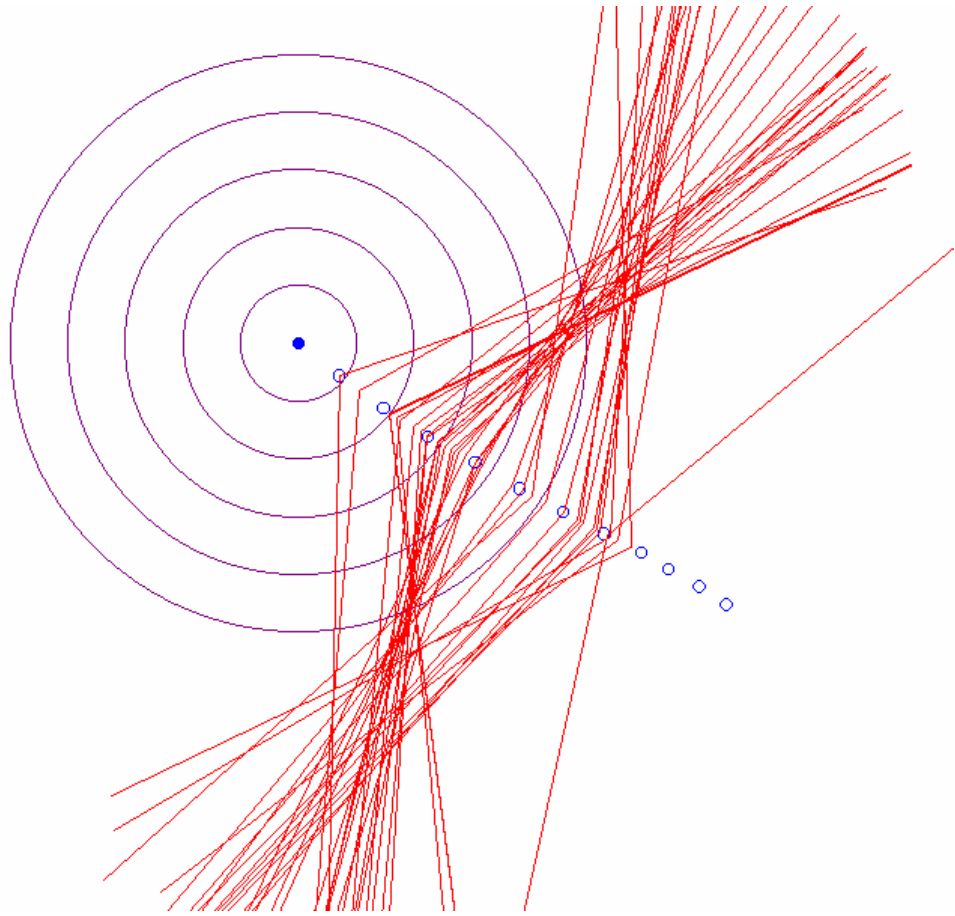


Figure 11. Whaltrak plot of angles obtained from a dolphin school with a 'loose' convergence suggesting a spread out group of dolphins that were likely traveling.

RECENT TECHNICAL MEMORANDUMS

Copies of this and other NOAA Technical Memorandums are available from the National Technical Information Service, 5285 Port Royal Road, Springfield, VA 22167. Paper copies vary in price. Microfiche copies cost \$9.00. Recent issues of NOAA Technical Memorandums from the NMFS Southwest Fisheries Science Center are listed below:

- NOAA-TM-NMFS-SWFSC-406 Preliminary estimates of cetacean abundance along the U.S. West Coast and within four National Marine Sanctuaries during 2005.
K.A. FORNEY
(June 2007)
- 407 Viability criteria for steelhead of the south-central and southern California coast.
D.A. BOUGHTON, P.B. ADAMS, E. ANDERSON, C. FUSARO,
E. KELLER, E. KELLEY, L. LENTSCH, J. NIELSEN, K. PERRY, H. REGAN,
J. SMITH, C. SWIFT, L. THOMPSON, and F. WATSON
(July 2007)
- 408 Logbook pilot program for California's nearshore groundfish fishery:
Results and lessons learned.
C. THOMSON, D. VenTRESKA, and D. COLPO
(August 2007)
- 409 AMLR 2006/2007 field season report: Objectives, Accomplishments,
and Tentative Conclusions.
J.D. LIPSKY, Editor
(September 2007)
- 410 Ichthyoplankton and station data for oblique (bongo net) plankton tows
taken during a survey of shallow coastal waters of the southern
California bight in 2004 and 2005.
W. WATSON, S.M. MANION, and R.L. CHARTER
(September 2007)
- 411 Spawning biomass of Pacific sardine (*Sardinops sagax*) off California
in 2007.
N.C.H. LO, B.J. MACEWICZ, and R.L. CHARTER
(November 2007)
- 412 Updated estimates of mortality and injury of cetaceans in the Hawaii-
based longline fishery, 1994-2005.
K.A. FORNEY and D.R. KOBAYASHI
(November 2007)
- 413 Assessment of the Pacific sardine resource in 2007 for U.S. Management
in 2008.
K.T. HILL, E. DORVAL, N.C.H. LO, B.J. MACEWICZ, C. SHOW and
R. FELIX-URAGA
(December 2007)
- 414 U.S. Pacific marine mammal stock assessments: 2007.
J.V. CARRETTA, K.A. FORNEY, M.S. LOWRY, J. BARLOW, J. BAKER,
B. HANSON, and M.M. MUTO
(December 2007)
- 415 California current ecosystem survey 2006 acoustic cruise reports for
NOAA FSV Oscar Dyson and NOAA FRV David Starr Jordan
G.R. CUTTER, JR., Editor and D.A. DEMER
(January 2008)

